Overview of the Summer 2004 Intercontinental Chemical Transport Experiment–North America (INTEX-A)

JOURNAL OF GEOPHYSICAL RESEARCH, VOL. 111, D24S01, doi:10.1029/2006JD007905, 2006

Overview of the summer 2004 Intercontinental Chemical Transport Experiment–North America (INTEX-A)

H. B. Singh,[1] W. H. Brune,[2] J. H. Crawford,[3] D. J. Jacob,[4] and P. B. Russell[1]

Received 10 August 2006; revised 31 October 2006; accepted 8 November 2006; published 16 December 2006.

[1] The INTEX-A field mission was conducted in the summer of 2004 (1 July to 15 August 2004) over North America (NA) and the Atlantic in cooperation with multiple national and international partners as part of a consortium called ICARTT. The main goals of INTEX-A were to (1) characterize the composition of the troposphere over NA, (2) characterize the outflow of pollution from NA and determine its chemical evolution during transatlantic transport, (3) validate satellite observations of tropospheric composition, (4) quantitatively relate atmospheric concentrations of gases and aerosols with their sources and sinks, and (5) investigate aerosol properties and their radiative effects. INTEX-A primarily relied on instrumented DC-8 and J-31 aircraft platforms to achieve its objectives. The DC-8 was equipped to measure detailed gas and aerosol composition and provided sufficient range and altitude capability to coordinate activities with distant partners and to sample the entire midlatitude troposphere. The J-31 was specifically focused on radiative effects of clouds and aerosols and operated largely in the Gulf of Maine. Satellite products along with meteorological and 3-D chemical transport model forecasts were integrated into the flight planning process. Intercomparisons were performed to quantify the accuracy of data and to create a unified data set. Satellite validation activities principally focused on Terra (MOPITT, MODIS, and MISR), Aqua (AIRS and MODIS) and Envisat (SCIAMACHY) to validate observations of CO, NO_2, HCHO, H_2O, and aerosol. Persistent fires in Alaska and NW Canada offered opportunities to quantify emissions from fires and study the transport and evolution of biomass burning plumes. Contrary to expectations, several pollution plumes of Asian origin, frequently mixed with stratospheric air, were sampled over NA. Quasi-Lagrangian sampling was successfully carried out to study chemical aging of plumes during transport over the Atlantic. Lightning NO_x source was found to be far larger than anticipated and provided a major source of error in model simulations. The composition of the upper troposphere was significantly perturbed by influences from surface pollution and lightning. Drawdown of CO_2 was characterized over NA and its atmospheric abundance related to terrestrial sources and sinks. INTEX-A observations provide a comprehensive data set to test models and evaluate major pathways of pollution transport over NA and the Atlantic. This overview provides a context within which the present and future INTEX-A/ICARTT publications can be understood.

Citation: Singh, H. B., W. H. Brune, J. H. Crawford, D. J. Jacob, and P. B. Russell (2006), Overview of the summer 2004 Intercontinental Chemical Transport Experiment–North America (INTEX-A), *J. Geophys. Res.*, *111*, D24S01, doi:10.1029/2006JD007905.

1. Introduction

[2] Rapid industrialization and the associated energy consumption have been major drivers of changes in atmospheric composition and climate [*Houghton et al.*, 2001]. In recent decades a mounting body of atmospheric data has shown that gas and aerosol pollutants are routinely transported on intercontinental scales and can influence air quality and regional climate in downwind regions [*Holloway et al.*, 2003; *Stohl*, 2004]. Independent studies have documented the transport of North American pollution to Europe [*Stohl and Trickl*, 1999; *Huntrieser et al.*, 2006; *Derwent et al.*, 2006; *Guerova et al.*, 2006]; Asian pollution to North America [*Jaffe et al.*, 1999; *Jacob et al.*, 1999; *VanCuren*, 2003]; Asian pollution to Europe [*Lelieveld et al.*, 2002; *Grousset et al.*, 2003], and North American and European pollution to Asia [*Liu et al.*, 2002; *Wild et al.*, 2004]. Observational data have shown that the surface O_3

[1]NASA Ames Research Center, Moffett Field, California, USA.
[2]Department of Meteorology, Pennsylvania State University, University Park, Pennsylvania USA.
[3]NASA Langley Research Center, Hampton, Virginia, USA.
[4]Division of Applied Sciences, Harvard University, Cambridge, Massachusetts, USA.

0148-0227/06/2006JD007905$09.00

Table 1. Principal Mobile Platforms in Operation During the Summer 2004 ICARTT Study

Platform Type	Study Name	Platforms (Country)	Dates of Operation (2004)	Bases of Operation[a]	Nominal Specifications, km	
					Altitude	Range
Airborne	INTEX-A	NASA DC-8[b] (United States)	1 Jul to 15 Aug	DR, MA, PT	0.2–12.5	9000
Airborne	INTEX-A	NASA/Sky Research J-31[c] (United States)	12 Jul to 8 Aug	PT	0.1–7.5	1500
Airborne	NEAQS-ITCT	NOAA WP-3D[b] (United States)	1 Jul to 15 Aug	PT	0.1–7.5	6000
Airborne	NEAQS-ITCT	NOAA DC-3[b] (United States)	1 Jul to 15 Aug	PT	0.1–3.6	1500
Airborne	NEAX	DOE G-1[b] (United States)	19 Jul to 15 Aug	LT	0.3–7.5	2000
Airborne	AIF	CIRPAS Twin Otter[c] (United States)	2–20 Aug	CL	0.1–3.1	500
Airborne	ITOP	NERC BAe146-300[b] (UK)	4 Aug to 8 Aug	AZ	0.1–10.5	2000
Airborne	ITOP	DLR Falcon-20[b] (Germany)	5 Jul to 6 Aug	OB, CR	0.1–12.8	3500
Airborne	CTC-TIMS	NRC-IAR Convair 580[c] (Canada)	21 Jul to 18 Aug	CL	0.1–7.5	5000
Surface[d]/ship	NEAQS-ITCT	NOAA R/V *Ronald H. Brown* (United States)	5 Jul to 13 Aug	Gulf of Maine	surface	21000
Spaceborne[e]	Terra-NASA	Terra (MOPITT, MISR, MODIS) (United States)	all year	space	all altitudes	global coverage
Spaceborne[e]	Aqua-NASA	Aqua (AIRS, MODIS) (United States)	all year	space	all altitudes	global coverage
Spaceborne[e]	Envisat-ESA	Envisat (SCIAMACHY) (European Union)	all year	space	all altitudes	global coverage

[a]DR, Dryden Flight Research Center, California (34.9°N, 117.9°W); MA, Mid-America/Mascoutah, Illinois (38.5°N, 89.8°W); PT, Pease International Tradeport, New Hampshire (43.1°N, 70.8°W); LT, Latrobe, Pennsylvania (40.3°N, 79.4°W); CL, Cleveland, Ohio (41.3°N, 81.4°W); AZ, Azores, Portugal (38.6°N, 28.7°W); OB, Oberpfaffenhofen, Germany (48.1°N, 11.3°E); CR, Creil, France (49.3°N, 2.5°E).

[b]Extensive payload principally designed to study atmospheric composition and chemistry. DC-8 and DC-3 also contained ozone/aerosol lidar.

[c]J-31 payload (see text) was principally designed to study aerosols, clouds, and radiation and Convair and Twin Otter to study aerosols and clouds.

[d]A number of fixed surface stations and sonde release sites also operated during this experiment. See *Fehsenfeld et al.* [2006] for a detailed overview of these.

[e]Principal focus was on chemical measurements in the troposphere.

mixing ratios of air entering Europe and NA may have increased by 0.3–0.5 ppb yr^{-1} over the last two decades [*Lin et al.*, 2000; *Jaffe et al.*, 2003; *Parrish et al.*, 2004; *Simmonds et al.*, 2004; *Vingarzan*, 2004; *Oltmans et al.*, 2006]. The direct and indirect radiative effects of aerosols on clouds are also an important area of investigation [*Houghton et al.*, 2001]. During the last decade the NASA (acronyms are defined at the end of this paper) tropospheric chemistry program has investigated the outflow of pollution from the Asian continent to the Pacific Ocean [*Hoell et al.*, 1996, 1997; *Raper et al.*, 2001; *Jacob et al.*, 2003]. INTEX-North America (NA) was a major NASA led integrated field experiment that focused on the inflow and outflow of pollution over the North American continent with the goal of understanding the transport and transformation of gases and aerosols on transcontinental/intercontinental scales [*Singh et al.*, 2002]. The first phase of INTEX-NA (INTEX-A) was completed in the summer of 2004 and forms the basis of this special section.

[3] INTEX-A was an integrated mission performed over NA and the Atlantic during the summer of 2004 in cooperation with multiple national and international partners under a consortium called ICARTT (http://cloud1.arc.nasa.gov/intex-na/; http://www.al.noaa.gov/ICARTT/). This effort had a broad scope to investigate the transport and chemistry of long-lived greenhouse gases, oxidants and their precursors, aerosols and their precursors, as well their relationship with radiation and climate. NASA's DC-8 and J-31 were joined by aircraft from a large number of European and North American partners (Table 1) to explore the composition of the troposphere over NA and the Atlantic as well as radiative properties and effects of clouds and aerosols in a coordinated manner. An important new advance has been the launch of new satellite instruments that have the capability to map pollution in the troposphere on regional to global scales [*Borrell et al.*, 2004; *Schoeberl et al.*, 2004; *Richter et al.*, 2005]. INTEX-A performed the dual role of validating satellite observations of tropospheric composition as well as integrating them with in situ observations. Specific sampling goals were achieved with the aid of chemical transport model (CTM) forecasts and a meteorological support system that allowed targeted sampling of air parcels with desired characteristics.

[4] INTEX-A/ICARTT was organized around a few major objectives aimed at (1) characterizing the large-scale composition of the NA troposphere, (2) characterizing the outflow of pollution from NA and determining its chemical evolution during transatlantic transport, (3) validating satellite observations of tropospheric composition, (4) quantitatively relating atmospheric concentrations of gases and aerosols with their sources and sinks, and (5) investigating aerosol radiative properties and their effects. Summer season was selected because it is a season that is photochemically active, biogenic emissions and boreal fires are at their peak, and aerosol radiative forcing is near its maximum. Cold fronts and warm conveyor belts, while reduced in frequency in summer, continue to lift surface pollution to the free troposphere where it can be carried by the prevailing westerlies toward the European continent. INTEX-A aimed to better understand the chemical and physical processes that control the evolution of pollution during transatlantic transport, provide the advantage of improved source characterization offered by concurrent measurements of a large number of chemical species, relate radiative and chemical properties, and ultimately improve predictive capabilities via accurate model simulations.

[5] Although several field experiments have been performed over NA in the past decades and results published and evaluated in special issues of journals [see *Fehsenfeld et al.*, 1996; *Singh et al.*, 1999; *Russell et al.*, 1999; *Schere et al.*, 2000], this was the most complex and integrated study done to date that spanned the midlatitudes from the eastern Pacific to the eastern Atlantic and permitted sampling of the entire troposphere over NA. This overview focuses mainly on the goals and activities of the NASA DC-8 and J-31 aircraft during the summer 2004 study.

2. Mission Design and Implementation

2.1. Measurement Platforms

[6] The principal mobile platforms that participated in the INTEX-A/ICARTT campaign, their bases of operation,

Table 2a. DC-8 Science Payload During INTEX-A[a]

Parameters	Method	Principal Investigators	Detection Limit/Response (Nominal Accuracy)
O_3	NO/O_3 chemiluminescence	M. Avery, NASA LaRC	1 ppb/1 s (±5%)
O_3 and aerosol profile	UV DIAL lidar	E. Browell, NASA LaRC	–/60 s (±10%)
NO, NO_2, HCHO	LIF	D. Tan, Georgia Institute of Technology	5 ppt/60 s (±10%), 15 ppt/60 s (±10%)
NO_2, NO_y	LIF and thermal dissociation	R. Cohen, University of California, Berkeley	1 ppt/60 s (±10%), 10 ppt/60 s(±10%)
PANs, OVOC, nitriles	GC-ECD/PID/RGD	H. Singh, NASA ARC	1 ppt/90 s (±15%), 10 ppt/120 s (±20%)
HNO_3, H_2O_2, organic acids	CIMS	P. Wennberg, California Institute of Technology	5 ppt/10 s (±15%)
H_2O_2, CH_3OOH, HCHO	derivative HPLC and fluorescence	B. Heikes, University of Rhode Island	20 ppt/150 s (±20%)
HCHO	TDL absorption spectrometry	A. Fried, NCAR	20 ppt/60 s (±10%)
OH, HO_2, naphthalene	LIF	W. Brune, Pennsylvania State University	0.01, 0.2, 10 ppt/20 s (±15%)
SO_2, HNO_4	CIMS	G. Huey, Georgia Institute of Technology	5 ppt/15 s (±15%)
NMHC, halocarbons, alkyl nitrates	whole air samples; GC- FID/EC/MS	D. Blake, University of California, Irvine, and E. Atlas, University of Miami	1 ppt/100 s (±2–10%)
CO, CH_4, N_2O	TDL absorption spectrometry	G. Sachse, NASA LaRC	1 ppb/5 s (±5%)
CO_2	nondispersive infrared	S. Vay, NASA LaRC	0.1 ppm/1 s (±0.1%)
H_2O	open path TDL absorption spectrometry	G. Diskin, NASA LaRC; J. Podolske, NASA ARC	0.1 ppm/1 s (±5%)
H_2O, $J(NO_2)$	cryogenic hygrometer, filter radiometer	J. Barrick, NASA LaRC	5 ppm/10 s (±10%), 10^{-6} s/20 s (±10%)
Aerosol bulk ionic composition	particle into liquid sampling (PILS)/IC	R. Weber, Georgia Institute of Technology	5 ppt/150 s (±15%)
Bulk aerosol composition, HNO_3	mist chamber/IC	R. Talbot, University of New Hampshire	10 ppt/300 s (±15%)
Aerosol number, size, composition, microphysics, optical properties, light absorption and scattering, cloud water content	particle spectrometers, volatility TDMA, CN counters, nephelometer, soot photometer, f(RH), cloud and aerosol probes	A. Clarke, University of Hawaii, and B. Anderson, NASA LaRC	
Actinic fluxes and photolytic frequencies	spectral radiometry, zenith and nadir	R. Shetter, NCAR	10^{-8} s/15 s (±5%)

[a]Instruments on board the DC-8 and J-31 also measured pressure, temperature, dew point, aircraft position and orientation.

campaign duration, and specifications are summarized in Table 1. Approximately 9 aircraft participated in this study for extended periods of time. One other aircraft (NSF Wyoming King Air) had a more limited role in this study and is not included in Table 1. These airborne platforms had the capability to sample much of the midlatitude troposphere over long distances. The bases of operation were selected to facilitate sampling over NA and during transatlantic transport. Complementing these airborne platforms were several fixed surface air quality stations that operated during this study and in some cases continued to collect data after the study to develop more robust statistics. Principal among these were several air quality ground stations located in New Hampshire, Chebogue Point (Canada), and Pico (Azores). The NOAA ship R/V *Ronald H. Brown* also focused on the boundary layer outflow of pollution in the Gulf of Maine.

[7] Data were also available from several satellites overhead both in real time and for post mission analysis. Satellite observations both guided flight planning and helped to extend the range of airborne observations. In return, the airborne measurements provided validations of satellite observations. Integration of data from these multiple platforms was one of the central goals of this study. The INTEX Ozonesonde Network Study (IONS), organized by pooling resources from Environment Canada, NASA, and NOAA, provided some 300 O_3 profiles from 11 fixed stations and the R/V *Ronald H. Brown* [*Thompson et al.*, 2006a, 2006b]. The IONS network covered a wide region over NA that extended from 30 to 45°N and 60 to 125°W. Ozonesondes were released on a daily basis from three fixed sites and the R/V *Ronald H. Brown* and 1–3 times a week from other stations. Additional details about these platforms are available from http://cloud1.arc.nasa.gov/intex-na/ and http://www.al. noaa.gov/ICARTT/.

2.2. Instrument Payload and Measurement Capability

[8] The payloads of a majority of airborne platforms in Table 1 (e.g., DC-8, WP-3D, G-1, BAe-146, Falcon) were designed to measure detailed gas and aerosol composition in the troposphere. Three aircraft (J-31, Twin Otter, and Convair) were more focused on radiative and microphysical properties of clouds and aerosols. The DC-8 and the J-31 had an additional role that involved validation of satellite measurements of gases and aerosol optical properties in the troposphere. Table 2a shows the DC-8 payload of in situ and remote sensors for measurements of both gases and aerosols. Major greenhouse gases, ozone and precursors, aerosols and precursors, and a large number of tracers were measured. Detailed VOC, OVOC, and reactive nitrogen (NO_x, HNO_3, HO_2NO_2, PAN) speciation was carried out. A large number of tracers that could be used to identify specific sources such as biomass combustion (HCN, CH_3CN), biogenic emissions (isoprene), anthropogenic emissions (CO, halocarbons), and oceanic emissions ($CHBr_3$) were measured. A nadir and zenith viewing UV lidar measured O_3 and aerosols remotely. HO_x (OH and

Table 2b. J-31 Science Payload During INTEX-A[a]

Parameters	Method	Principal Investigators	Detection Limit/Response (Nominal Accuracy)
Optical depth, water vapor column	tracking Sun photometer, 354–2138 nm	P. Russell, NASA ARC	slant OD ~0.002/3 s (±0.01), slant WV ~0.0005 to 0.006 cm^{-1}/3 s (±10%)
Solar spectral flux	spectrometer (380–1700 nm) with nadir and zenith hemispheric collectors	P. Pilewskie, University of Colorado	absolute accuracy 3–5%, precision 1%/0.25 s

[a]Instruments on board the DC-8 and J-31 also measured pressure, temperature, dew point, aircraft position and orientation.

HO_2) free radicals, that are critical to understanding oxidative processes, were directly measured along with their precursors (peroxides and aldehydes). Spectral radiometers allowed direct measurement of actinic flux used to derive key photolysis frequencies. Multiple instruments measured physical, chemical, and optical properties of fine and coarse aerosol. While many of the instruments had previously flown aboard the DC-8, several new instruments were incorporated. Two new CIMS instruments were used to measure HO_2NO_2 and SO_2 [*Huey et al.*, 2006] and hydrogen peroxide [*Crounse et al.*, 2006]. A new LIF instrument measured NO_2 as well as total PANs and total alkyl nitrates via their thermal decomposition to NO_2 [*Day et al.*, 2002]. INTEX-A provided the first in situ measurements of HO_2NO_2 [*Huey et al.*, 2006] and peracetic acid (J. Crounse et al., Peroxyacetic acid is ubiquitous in the upper troposphere, submitted to *Geophysical Research Letters*, 2006, hereinafter referred to as Crounse et al., submitted manuscript, 2006) in the troposphere.

[9] Specific science objectives of the J-31 included validating satellite retrievals of Aerosol Optical Depth (AOD) spectra and of water vapor columns, measuring aerosol effects on radiative energy fluxes, and characterizing cloud properties using visible and near infrared reflectance in the presence of aerosols. To achieve these objectives, the J-31 carried two instruments (Table 2b) that operated in close coordination with measurements by other platforms especially the DC-8 and the R/V *Ronald H. Brown*. The Ames Airborne Tracking Sunphotometer (AATS) measured aerosol and water vapor attenuation of the direct beam from the Sun. The Solar Spectral Flux Radiometer (SSFR) measured solar energy from all directions with sensors looking both above and below the aircraft. Both AATS and SSFR covered a wide range of wavelengths, from the ultraviolet, through the visible, and into the near infrared.

[10] Satellite instruments are becoming capable of air chemistry measurements in the troposphere and received a great deal of attention from the NASA DC-8 and the J-31 platforms. In INTEX-A our principal focus was on the CO vertical profiles obtained by AIRS and MOPITT, NO_2 and HCHO trop-columns from SCIAMACHY, and aerosol columns from MODIS-Terra, MODIS-Aqua, and MISR (Table 3). Additional details about the payloads of other platforms listed in Table 1 have been summarized by *Fehsenfeld et al.* [2006].

2.3. Flight Planning and Execution

[11] Satellite observations, along with meteorological and chemical forecasts from global and regional models were extensively used to plan, coordinate, and implement the INTEX-A field mission. Table 4 lists the major CTMs in use for planning this experiment. Meteorological products were derived from the NCEP reanalysis data (H. E. Fuelberg et al., Meteorological conditions and anomalies during INTEX-NA, submitted to *Journal of Geophysical Research*, 2006, hereinafter referred to as Fuelberg et al., submitted manuscript, 2006). Daily meteorological and chemical forecasts guided the design and execution of the mission. Typical model products included source-tagged CO tracers, aerosol tracers, O_3, and PAN distributions. Meteorological products included satellite imagery (visible, infrared, and water channels), precipitation and cloud fields, backward and forward trajectories and multi day synoptic weather forecasts. Principal satellite instruments that provided near real-time data to guide flight planning were AIRS and MOPITT (CO columns), SCIAMACHY (NO_2 columns), MODIS and AVHRR (aerosol, fire counts), and TOMS (tropospheric O_3, absorbing aerosols). To monitor lightning activity, real-time data from the NLDN and LRLN were provided by the Global Hydrology and Climate Center at NASA Marshall Space Flight Center. These data were combined with forward trajectories by groups at Florida State and NASA Goddard to assess lightning influence for flight planning purposes.

[12] The DC-8 science activities were closely coordinated with the main air quality (WP-3D, BAe 146, and Falcon) and radiation (J-31) platforms. This coordination was necessary to accomplish intercomparisons among instruments, to achieve several objectives that were unattainable by a single platform, and to collect complementary data where appropriate. The bases of operation of these platforms

Table 3. Satellite Measurements Targeted for Validation in INTEX-A[a]

Satellite Instruments	Platform (Launch Date)	Validation Measurements	More Information
MISR	Terra (Dec 1999)	aerosol	http://terra.nasa.gov/About/MISR/index.php
MODIS	Terra (Dec 1999)	aerosol, H_2O	http://terra.nasa.gov/About/MODIS/index.php
MOPITT	Terra (Dec 1999)	CO	http://terra.nasa.gov/About/MOPITT/index.php
AIRS	Aqua (May 2002)	CO, H_2O	http://aqua.nasa.gov/about/instrument_airs.php
MODIS	Aqua (May 2002)	aerosol, H_2O	http://aqua.nasa.gov/about/instrument_modis_science.php
SCIAMACHY	Envisat (Mar 2002)	NO_2, HCHO	http://www.iup.physik.uni-bremen.de/sciamachy/

[a]All validations were performed with instruments looking in the nadir.

Table 4. Models Used for Flight Forecasting and Analysis in INTEX-A[a]

Model	Type	Resolution: Horizontal	Resolution: Vertical Levels	Underlying Meteorological Model	Chemical Package	Principal Investigator	Additional References
GEOS-4	global	1° × 1.25°	55	GEOS-4	tagged tracers	D. J. Jacob, Harvard	
GEOS-Chem	global	2° × 2.5°	55	GEOS-4	ozone-NO_x-VOC-aerosol chemistry	D. J. Jacob, Harvard	Hudman et al. (submitted manuscript, 2006)
MOZART-4-GFDL	global	1.9° × 1.9°	64	NCEP/GFS forecast	C_1–C_{10} detailed NMHC chemistry; tagged tracers	L. W. Horowitz, NOAA/GFDL	*Horowitz et al.* [2003]
MOZART-4-NCAR	global	2.8° × 2.8°	28	NCAR/NCEP reanalysis	C_1–C_{10} detailed NMHC chemistry; tagged tracers	L. K. Emmons, NCAR	*Pfister et al.* [2005]
RAQMS	global	2° × 2.5°	36	NCEP	C_1–C_7 detailed NMHC chemistry; tagged tracers	R. B. Pierce, NASA Langley	*Pierce et al.* [2003]
STEM	regional	4 × 4 km to 80 × 80 km	21	MM5 or RAMS	C_1–C_7 detailed NMHC chemistry; tagged tracers	G. R. Carmichael, University of Iowa	*Tang et al.* [2004]
Photochemical model/LaRC	box	. . .	. . .	. . .	C_1–C_7 detailed NMHC chemistry	J. H. Crawford, NASA Langley	*Crawford et al.* [1999]

[a]Flight planning process also used weather forecasts based on NCEP analysis and near real-time satellite data from AIRS and MOPITT (CO columns), MODIS and AVHRR (aerosol, fire counts), TOMS (tropospheric ozone, absorbing aerosols), and LIS (lightning). Potential vorticity and convective influence plots were also available.

(Table 1) were selected to sample North American atmospheric composition and transatlantic transport. In many cases quasi-Lagrangian studies were carried out when pollution plumes sampled over NA were subsequently sampled over the central and eastern Atlantic after several days of transport [*Law et al.*, 2005; *Methven et al.*, 2006].

2.4. Flight Tracks and Sampled Air Masses

[13] Figure 1 shows the flight tracks of four major air quality platforms (DC-8, WP-3D, BAe-146, Falcon-20) and the radiation platform (J-31) that collectively covered an area from the eastern pacific to the eastern Atlantic. Each flight was carefully planned to achieve the INTEX-A targeted objectives of investigating outflow of gases and aerosols, source characterization, chemical evolution, direct/indirect effects of aerosols, satellite validation, and instrument intercomparisons. The DC-8 flew 170 hours in 18 science flights of 7–10 hour duration from its three bases of operation in Table 5a. The DC-8 started from the west coast of the United States and sampled air masses over the Pacific before moving to mid-America and ultimately joined other platforms at the eastern site. Figure 2 shows the DC-8 flight tracks for each of the science flights. The J-31 flew 60 hours in shorter science flights of 2–4 hour duration operating exclusively from the New Hampshire site. Tables 5a and 5b provide a brief summary of the flight objectives of each of the DC-8 and J-31 flights with more details available at http://cloud1.arc.nasa.gov/intex-na/flight_reps.html. Figure 3 is a plot of CO and O_3 that clearly shows that air masses influenced by forest fires, anthropogenic pollution, and stratosphere were sampled during INTEX-A.

2.5. Intercomparisons

[14] Intraplatform and interplatform comparisons of measurements were extensively performed to establish accuracies and precisions. On the DC-8 itself, several chemical measurements were duplicated using a variety of different techniques (Table 2). Salient among these were measurements of O_3, H_2O, HCHO, H_2O_2, HNO_3, NO, and aerosol composition. Intercomparisons were also performed with other aircraft by coflying these in formation with a separation of less than 300 m in the horizontal and 100 or so meters in the vertical. Two to three levels were chosen between 0 and 8 km altitudes and the entire intercomparison including descent and ascent typically lasted one hour. Table 6 provides a summary of the intercomparisons carried out by the DC-8. The BAe 146 separately intercompared with the DLR Falcon-20 based on the European continent.

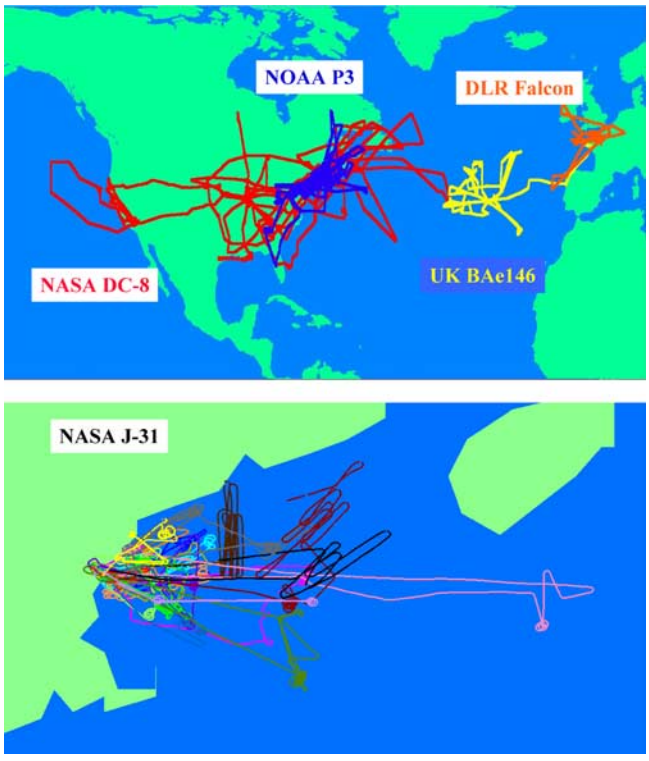

Figure 1. INTEX-ICARTT flight tracks of multiple platforms studying (top) air chemistry and (bottom) radiation. Figure 1 (top) is bounded by latitude 10–70°N, longitude 150°W–15°E, and Figure 1 (bottom) is bounded by latitude 41–45°N, longitude 290–296°W.

Table 5a. INTEX-A DC-8 Missions and Salient Activity[a]

Flight	Date	Operational Base[b]	Flight Hours	Salient Mission Activity
1–2	26–29 Jun 2004	NASA Dryden Flight Research Center (DFRC)	10.5	test flights, no chemical data archival required
3	1 Jul 2004	NASA DFRC	8.5	AIRS validation, characterization of low-level California and high-level Asian outflow, background and inflow characterization, and stratospheric intrusions
4	6 Jul 2004	NASA DFRC to Mid-America Airport	7.4	California plume transported to the east, Arizona fire plumes, frontal crossings over midwest and convective outflow over Great Plains
5	8 Jul 2004	Mid-America Airport	8.9	validation of the MOPITT and MODIS instruments aboard the Terra satellite, characterization of aged California outflow, mapping of midwestern boundary layer pollution, sampling of deep convection over the Carolinas, and exploring the relationship between biogenic emissions and their products over the Smoky Mountains
6	10 Jul 2004	Mid-America Airport	8.7	validation of instruments aboard the Envisat (SCIAMACHY) and Aqua (AIRS, MODIS) satellites, mapping of midwestern boundary layer pollution, sampling of deep convection, exploring the relationship between biogenic emissions and their products, and characterization of outflow from Texas
7	12 Jul 2004	Mid-America Airport	9.1	boundary layer mapping of south-central United States, aged convective/lightning outflow over southeast United States and validation of Park Falls FTS, SCIAMACHY, and AIRS
8	15 Jul 2004	Mid-America Airport to Pease International Tradeport Airport (ITA)	7.5	validation of Terra (MOPITT, MISR) and Aqua (AIRS, MODIS) instruments, validation of FTS CO2 column measurements at Park Falls, CO_2 intercomparison with the NSF King Air aircraft, characterization of Asian pollution, Alaskan fires, and anthropogenic pollution
9	18 Jul 2004	Pease ITA	9.1	validation of Envisat (SCIA) and Aqua (AIRS, MODIS) satellite instruments, a first attempt at the Lagrangian experiment, characterization of North American pollution outflow, characterization of Alaskan fires, and a flyby over the NOAA ship *Ronald H. Brown*
10	20 Jul 2004	Pease ITA	7.9	validation of Aqua (AIRS, MODIS)instruments, characterization of smoke from Alaskan fires transported over the United States, boundary layer pollution over the southeast and midwest
11	22 Jul 2004	Pease ITA	8.9	sampling polluted boundary layer outflow along the eastern seaboard both to the north and south of Pease; intercomparison between the NASA DC-8 and NOAA WP-3D aircraft; a coordinated validation profile with the J-31 over the NOAA research vessel *Ronald H. Brown* and beneath the MISR instrument on NASA's Terra satellite
12	25 Jul 2004	Pease ITA	9.3	convective outflow from southeast United States, map Ohio River Valley emissions in northerly flow and Terra underflight
13	28 Jul 2004	Pease ITA	10.2	sample the structure and chemical evolution of the U.S. continental outflow over the Atlantic and a comparison between the measurements on the DC-8 and the BAe146
14	31 Jul 2004	Pease ITA	9.0	satellite underpass, aged air sampling/recirculation, low-level outflow, DC-8/P-3 intercomparison, and possible Asian influences
15	2 Aug 2004	Pease ITA	9.5	underfly Terra (MOPITT/MODIS) and Aqua (AIRS) satellites, sample low-level North American outflow and aged air pollution aloft, conduct a coordinated closure experiment over *Ronald H. Brown* with the J-31, and a flyby over the ground Appledore island air quality station.
16	6 Aug 2004	Pease ITA	9.4	Continental outflow, city plumes, boundary layer characterization, Terra underflight
17	7 Aug 2004	Pease ITA	8.5	underfly Terra (MOPITT/MISR) and perform a predefined maneuver in coordination with the J-31, *Ronald H. Brown* and MISR, sample North American outflow, a stratospheric intrusion, and perform P-3 intercomparison.
18	11 Aug 2004	Pease ITA to Mid-America Airport	8.5	Terra underpass, Aqua underpass, NA outflow and WCB lifting, frontal crossing and low-level pollution
19	13 Aug 2004	Mid-America Airport	8.6	satellite underpass and outflow from major industrial cities
20	14 Aug 2004	Mid-America Airport to NASA DFRC	7.9	satellite underpass, Asian outflow, and NA inflow

[a]More details on individual flights can be found at http://cloud1.arc.nasa.gov/intex-na/flight_reps.html.
[b]NASA DFRC, 34.9°N, 117.9°W; Mid-America Airport, 38.5°N, 89.8°W; Pease ITA, 43.1°N, 70.8°W.

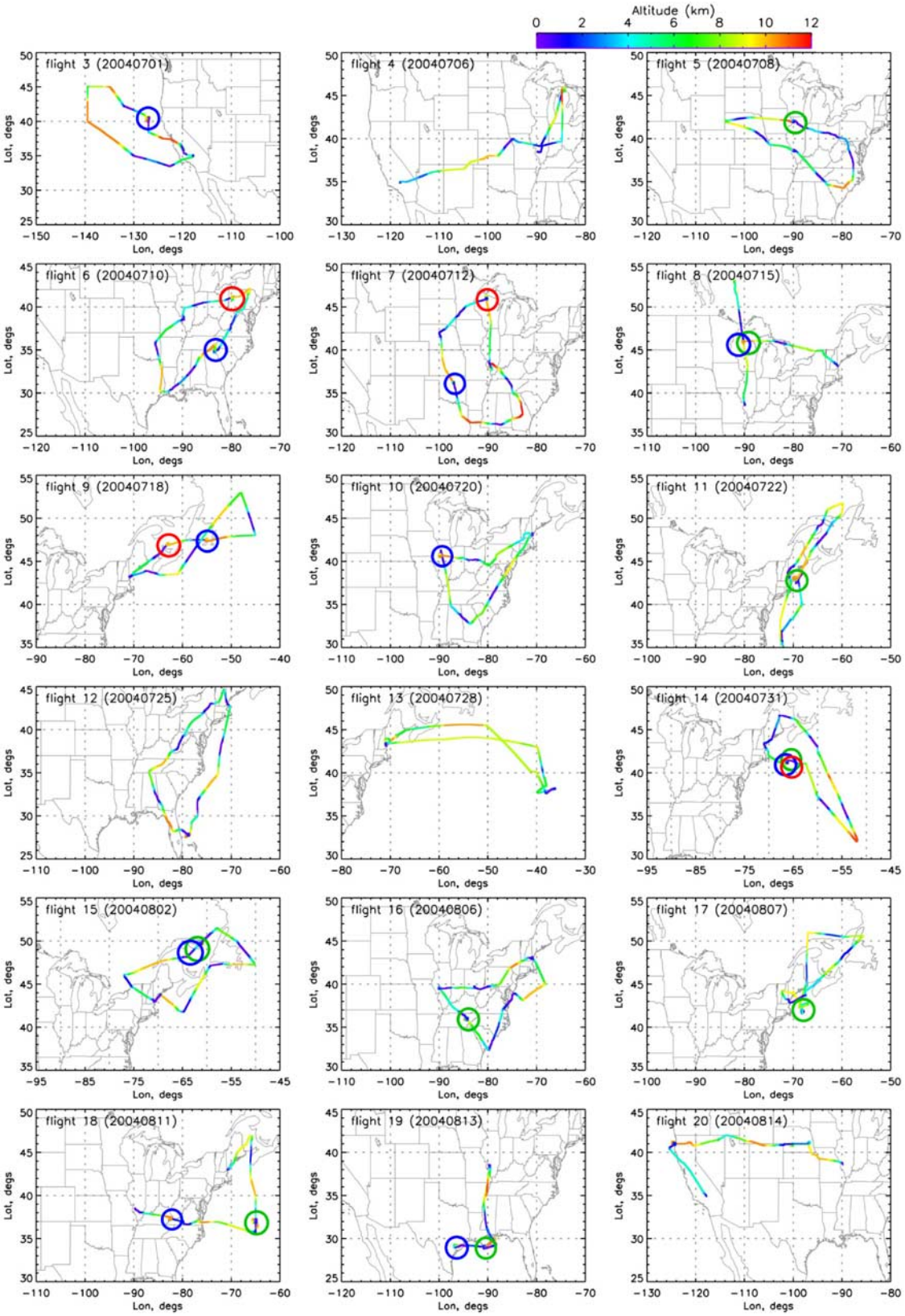

Figure 2. DC-8 flight tracks during INTEX-A. Circles indicate spirals designed for satellite validation for Aqua (blue), Terra (green), and Envisat (red).

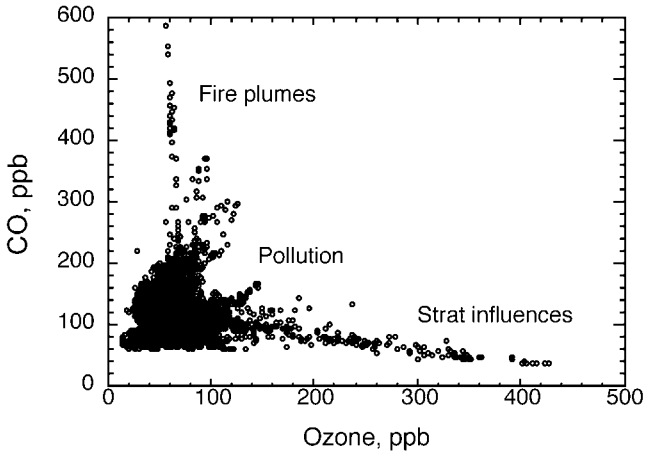

Figure 3. Fire plumes, anthropogenic pollution, and stratospheric influences sampled during INTEX-A.

The intercomparison data are available at http://www-air.larc.nasa.gov/missions/intexna/meas-comparison.htm.

2.6. Satellite Validation

[15] Satellites are increasingly able to measure key gases and aerosols in the troposphere. These sensors measure radiances from which information on atmospheric composition is retrieved using radiative transfer algorithms with substantial and often poorly characterized uncertainties. Validation with in situ vertical profiles is required, and this was a major activity during INTEX-A. The DC-8 focused on validation of CO, NO_2, H_2O, HCHO, and, together with the J-31, on aerosols and clouds (Table 3). Opportunities for satellite validation were sought daily during flight planning. Figure 2 shows all the satellite spirals undertaken by the DC-8. Specific times and locations for these spirals are given in Table 7. Validations were performed to test retrievals with a variety of underlying surfaces. A typical DC-8 validation flight involved measuring a profile from 0.2 to 11.5 km in about 20 km radius within ±30 min of the satellite overpass time under relatively cloud free conditions. This time coincidence was necessary for accurate

Table 5b. INTEX-A J-31 Missions and Salient Activity[a]

Flight	Date	Flight Hours	Salient Mission Activity
1–3	13 May 2004 and 9 Jul 2004	3.8	three test flights near NASA Ames
4–6	10 Jul 2004	11.9	three flights to transit Ames to Pease
7	12 Jul 2004	2.9	Aqua overpass at 1813 UT; good profile data, R/V *Ronald H. Brown* rendezvous
8	15 Jul 2004	3.0	over stratus clouds near *Ronald H. Brown* Terra overpass (1525 UT) and near surface Aqua (1705 UT); 2nd run above cloud past RB; two *Ronald H. Brown* sondes
9	16 Jul 2004	3.1	spiral descent and low-level legs around Aqua overpass time (1748 UT), increasing fog in the vicinity of low-level legs, profile near *Ronald H. Brown* for special sonde
10	17 Jul 2004	2.2	spiral descent and low-level legs around Terra overpass time (1513 UT), increasing Cirrus (Ci), about 5 min of Ci-free data, found *Ronald H. Brown* under Ci
11	20 Jul 2004	2.3	radiation legs over stratus near *Ronald H. Brown* with Terra overpass in MISR local mode swath; AOD profiles over stratus; brief AOD near surface
12	21 Jul 2004	2.7	low-level runs during Aqua OP at 1806 UT, two profiles in clear; aerosol gradient at several altitudes
13	22 Jul 2004	2.8	coordination with DC-8, *Ronald H. Brown*, and Terra in MISR local mode patch, collocated profile with DC-8 (18 min apart) over *Ronald H. Brown*
14	23 Jul 2004	1.9	aerosol profiles and near-surface legs with Aqua (1754 UT).
15	26 Jul 2004	2.0	Meteo and H_2O profiles over *Ronald H. Brown* near shore; cirrus or lower clouds for most of flight
16	29 Jul 2004	3.9	spiral descent profile over *Ronald H. Brown*, multiple low-level flybys of *Ronald H. Brown*, Terra MISR local mode, Aqua, two *Ronald H. Brown* sondes; aerosol gradient two ways
17	29 Jul 2004	4.3	successful airborne Langley flight at constant press alt (~6.4 km GPS) at sunset
18	31 Jul 2004	4.3	flew 297 nm E of Pease to find cirrus-free air; flew L-pattern at max alt of 20k ft, spiral down to 2k ft (status below), another L-pattern at 2k ft, and a final L-pattern at 7.5k ft above an aerosol layer; upon return, descent above *Ronald H. Brown* (3 miles offshore); *Ronald H. Brown* sonde; coordination with DC-3 lidar over *Ronald H. Brown*, but AATS got water vapor data only, because of cirrus
19	2 Aug 2004	2.5	Terra overpass; profile and legs in clear area; aerosol gradient two ways
20	2 Aug 2004	4.4	airborne Langley before descent to 200′, then low-level leg to *Ronald H. Brown*, ascent over *Ronald H. Brown* with its sonde, and continuation of airborne Langley
21	3 Aug 2004	2.4	coordination w/DC-3 w/legs at ~200′ and ~5200′, followed by *Ronald H. Brown* flyby and spiral ascent nearby with *Ronald H. Brown* sonde
22	7 Aug 2004	3.5	coordination w/DC-8, *Ronald H. Brown* and its sonde during Terra MISR local mode overpass; includes 5000′ and 200′ L-shaped legs and RB flybys, and spiral ascent w/DC-8
23	7 Aug 2004	5.0	airborne Langley before/after descent and ascent in clear air just east of *Ronald H. Brown* (~68.75°W, 43°N); post *Ronald H. Brown* Langley measurements were ENE of *Ronald H. Brown*; *Ronald H. Brown* sonde
24	8 Aug 2004	2.2	Aqua overpass at 1354 UT; very low AOD along extended 220′ run from 70°W to 68°W, 42.75°N; profiles down/up to 11,000′; level leg at 11,000′; ramped descent from 68°W to ~69°W
25	8 Aug 2004		aborted on runway
26	8 Aug 2004	3.0	airborne Langley E of Pease

[a]All J-31 science flights originated from the Pease ITA (43.1°N, 70.8°W). These are daytime flights. More details on individual flights can be found at http://cloud1.arc.nasa.gov/intex-na/flight_reps.html.

Table 6. Principal DC-8 Airborne Intercomparisons

Intercomparing Platforms	Dates (2004)	Approximate Location	Time, UT	Level Altitude Legs,[a] km
DC-8 and King Air	15 Jul	46°N, 90°W	1415–1515	spiral[b]
DC-8 and WP-3D	22 Jul	42°N, 68°W	1445–1530	4.4, 0.3
DC-8 and BAe146[c]	28 Jul	38°N, 38°W	1550–1702	6.8, 3.8, 0.2
DC-8 and WP-3D	31 Jul	45°N, 69°W	2252–2332	3.1, 0.6
DC-8 and WP-3D	7 Aug	44°N, 68°W	2133–2220	3.8, 0.3

[a]Aircraft flew in formation for the entire time during level legs, descent, and/or ascent.
[b]Centered on the WLEF Tall Tower (45.945°N, 90.273°W), the DC-8 and the King Air spiraled down from 11 to 0.1 km and 8 to 0.1 km, respectively.
[c]The BAe146 also separately intercompared with the DLR Falcon.

validation and, in addition, provided a measurement of many chemical and physical parameters that could be used to improve satellite retrievals. In many cases it was possible to simultaneously validate multiple satellite sensors when the overpass times were similar and instrument swaths quite wide. In situ aerosol measurements on these DC-8 spirals have also been used to test aerosol retrievals from GOES (S. Kondragunta et al., unpublished manuscript, 2006). The satellite sensors of primary attention for the J-31 were MISR and MODIS (Table 3) and the focus was on validating satellite retrievals of AOD spectra and water vapor columns. Although the Aura satellite was launched in July 2004 and was not ready for validation, INTEX-A data for O_3-CO correlations were used subsequently for TES/Aura validation [*Zhang et al.*, 2006].

3. Overview of First Results

[16] We present here a brief overview and synthesis of the results presented in the first collection of INTEX-A/ICARTT papers assembled in this special section of *Journal of Geophysical Research* and published elsewhere to date. We primarily focus on the goals and activities of the NASA DC-8 and J-31 platforms. Complementary papers are also being published in a second special section of *Journal of Geophysical Research*: ICARTT/NA-Europe. The reader is referred to the specific papers for more information.

3.1. Long-Distance Transport of Pollution

[17] Fuelberg et al. (submitted manuscript, 2006) provide an overview of the meteorological environment during INTEX-A. Seven cold fronts passed Atlanta, GA during INTEX-A, the greatest number between 2000 and 2005. These fronts brought record low temperatures to portions of the Great Plains and south. Frontal passages over the northeast were above average and the short time interval between passages (averaging 4.6 days) precluded the formation of stagnant high-pressure centers that lead to pollution build up. The persistent high pressure over Alaska led to a record number of wildfires. Typically, the ridge transported the fire by-products southeastward toward the INTEX-A domain where they were sampled by the DC-8 during numerous flights. On some flights, forward trajectories and satellite imagery showed that the plumes were also carried to parts of Europe, Africa, and the Arctic. An analysis of cloud-to-ground lightning from 2003 to 2005 showed that both flash counts and horizontal patterns of lightning flashes during INTEX-A were similar to other years. Deep convection and lightning were important factors during INTEX-A. Analysis of data by *Kiley and Fuelberg* [2006] shows that midlatitude cyclones were capable of producing vertical transport as great or greater than much stronger cyclones.

3.1.1. Forest Fire Emissions and Transport

[18] The summer of 2004 was one of the largest fire seasons on record in NA because of persistent wildfires in the boreal forests of Alaska and Canada resulting from exceptionally warm and dry conditions. According to the U.S. National Interagency Fire Center (http://www.cidi.org/wildfire), more than 2.6 million hectares burned in Alaska in 2004, which represents more than 8 times the 10-year average and the highest burning on record. In western Canada the fire season was also well above the 10-year average. Smoke plumes from these fires were identified by several satellites from their aerosol and CO signatures thousands of miles downwind and fire influences were widespread. As a result, HCN and CH_3CN, both tracers of biomass combustion, were elevated nearly everywhere in the troposphere [*Singh et al.*, 2006]. The interception of biomass burning plumes several thousand kilometers downwind by the DC-8 observations indicated that very limited mixing was occurring between the stretching filaments and the background. Tracers such as CO and HCN reached concentrations as high as 600 ppb and 3 ppb in the mid Atlantic. The smoke particles were also transported efficiently from the source regions to Europe without major removal of particles. The availability of extensive atmospheric CO observations from aircraft and satellite for this period provided an opportunity to evaluate our understanding of factors controlling boreal fire emissions and their impact on atmospheric chemistry.

Table 7. DC-8 Satellite Validation Opportunities During INTEX-A

Satellite Underflown	Flight	Dates (2004)	Approximate Location	Time, UT
Aqua	3	1 Jul	41°N, 127°W	2128–2156
Terra	5	8 Jul	42°N, 90°W	1721–1755
Envisat	6	10 Jul	41°N, 80°W	1553–1622
Aqua	6	10 Jul	35°N, 83°W	1822–1855
Envisat	7	12 Jul	46°N, 90°W	1621–1647
Aqua	7	12 Jul	36°N, 97°W	1927–1952
Terra	8	15 Jul	46°N, 90°W	1723–1750
Envisat	9	18 Jul	47°N, 63°W	1446–1521
Aqua	9	18 Jul	48°N, 55°W	1619–1651
Aqua	10	20 Jul	41°N, 90°W	1855–1926
Terra	11	22 Jul	43°N, 70°W	1558–1636
Terra	12	25 Jul	28°N, 79°W	1629–1658
Aqua/Terra/Envisat	14	31 Jul	41°N, 66°W	1601–1627
Aqua/Terra	15	2 Aug	50°N, 61°W	1621–1648
Terra	16	6 Aug	36°N, 84°W	1624–1654
Terra	17	7 Aug	42°N, 68°W	1520–1546
Terra	18	11 Aug	37°N, 65°W	1502–1530
Aqua	18	11 Aug	37°N, 83°W	1834–1910
Terra	19	13 Aug	30°N, 89°W	1537–1614
Aqua	19	13 Aug	29°N, 91°W	1851–1950

[19] S. Turquety et al. (Inventory of boreal fire emissions for North America: Importance of peat burning and pyroconvective injection, submitted to *Journal of Geophysical Research*, 2006, hereinafter referred to as Turquety et al., submitted manuscript, 2006) constructed a daily bottom-up fire emission inventory, including consideration of peat burning and high-altitude (buoyant) injection, and evaluated it in a global CTM (GEOS-Chem) simulation of CO through comparison with MOPITT satellite and ICARTT aircraft observations. They estimate a total North American fire emission of 28.6 Tg-CO during the summer of 2004 consistent with the top-down estimate of 30 ± 5 Tg-CO derived by *Pfister et al.* [2005] from inverse modeling of MOPITT observations. The fires represented a major perturbation to summertime North American emissions of the same magnitude as the anthropogenic source (18 Tg CO). It was further deduced that the largest fires injected a significant fraction of their emissions in the upper troposphere (UT) that could be easily transported long distances.

[20] *Cook et al.* [2006] sought to investigate whether the fires in Alaska in 2004 were only of regional importance or had an impact on a wider, even hemispheric scale. They used the Cambridge TOMCAT model and the emissions data from Turquety et al. (submitted manuscript, 2006) and investigated the long-range transport of pollution across the North Atlantic and its impact on O_3 production. The simulated plumes closely match CO data from the aircraft and the MOPITT satellite instrument. Although uncertainties remain in the simulation of PAN and NO_x, TOMCAT simulations showed increased O_3 in the troposphere over much of NA, the north Atlantic, and western Europe from photochemical production and transport. Biomass burning plumes sampled by the DC-8 in the free troposphere over NA did not show this O_3 enhancement. R. C. Hudman et al. (A multiplatform analysis of the North American reactive nitrogen budget during the ICARTT summer intensive, submitted to *Journal of Geophysical Research*, 2006, hereinafter referred to as Hudman et al., submitted manuscript, 2006) attribute this to rapid conversion of the emitted NO_x to PAN.

[21] W. W. McMillan et al. (unpublished manuscript, 2006) investigated transport of CO from a large fire outbreak in the Alaskan/Canadian Yukon region on 11–14 July 2004 by following it downwind to the southeastern United States and Europe until 22 July 2004. Correlations between AIRS CO and MODIS AOD indicated changes in the vertical distribution of CO as supported by in situ measurements, meteorological data, and forward trajectory analyses. Ground based lidar observations showed smoke plume altitudes from 3 to 11 km over Wisconsin and 1 to 4 km over Maryland in agreement with the forward trajectories. Comparison of AIRS CO maps and forward trajectories from the fire locations illustrate the great variations in fire emissions, especially emission height, that must be accounted for if any forecast model is to correctly predict the impact of fire emissions days to weeks downwind.

[22] Aerosol measurements revealed statistically robust differences in aerosol size, composition, spectral optical properties, and humidity-dependent growth for fires compared to other sources (A. D. Clarke et al., Biomass burning and pollution aerosol over North America: Organic components and their influence on spectral optical properties and humidification response, submitted to *Journal of Geophysical Research*, 2006, hereinafter referred to as Clarke et al., submitted manuscript, 2006). Aerosol particles from fires were larger, had a greater fraction of organic carbon (OC), and had a lower growth in response to increasing humidity. They also exhibited unique spectral signatures that revealed that they could be separated optically using remote sensing approaches.

3.1.2. Asian Pollution Over North America

[23] Asian pollution transport to NA peaks in late spring and little influence in summer was expected from historical evidence. Contrary to this expectation, significant Asian pollution influences were encountered across NA. INTEX-A observations thus offered an unprecedented opportunity to quantify the role of transpacific transport of Asian pollution during summer. Asian air masses were identified via trajectory analysis, model simulations, and from their chemical composition. Q. Liang et al. (Summertime influence of Asian pollution in the free troposphere over North America, submitted to *Journal of Geophysical Research*, 2006, hereinafter referred to as Liang et al., submitted manuscript, 2006) identified five major Asian plumes sampled during INTEX-A and analyzed these observations to examine the summertime influence of Asian pollution in the free troposphere over NA. By applying correlation analysis and Principal Component Analysis (PCA) to the observations between 6 and 12 km, they find dominant influences from recent convection and lightning (13% of observations), Asia (7%), the lower stratosphere (7%), and boreal forest fires (2%), with the remaining 71% assigned to background. Typically Asian plumes contained high levels of CO, O_3, HCN, PAN, acetylene, benzene, methanol, and SO_4^-. The partitioning of reactive nitrogen species in the Asian plumes was dominated by PAN (~600 pptv), with varying NO_x/HNO_3 ratios in individual plumes consistent with different plume ages ranging from 3 to 9 days. Export of Asian pollution in warm conveyor belts of midlatitude cyclones, deep convection, and lifting in typhoons all contributed to the five major Asian pollution plumes. Liang et al. (submitted manuscript, 2006) point out that compared to past measurement campaigns of Asian outflow during spring, INTEX-A observations display unique characteristics: lower levels of anthropogenic pollutants (CO, propane, ethane, benzene) due to their shorter summer lifetimes; higher levels of biogenic tracers (methanol and acetone) because of a more active biosphere; as well as higher levels of PAN, NO_x, HNO_3, and O_3.

3.1.3. North American Pollution Outflow and Transatlantic Transport

[24] Air mass trajectories and model predictions were used to establish the occurrence of events where chemical processing could be studied in a quasi-Lagrangian framework. Several such opportunities were identified and aircraft were successfully flown to the forecast locations of the previously sampled air masses. ICARTT studies provided evidence that this type of experiment can be successfully performed in the free troposphere on intercontinental scales. Attempts were made to intercept and sample air masses several times during their journey across the North Atlantic using four aircraft based in New Hampshire (USA), Faial (Azores) and Creil (France). *Methven et al.* [2006] describe

techniques to identify Lagrangian matches between flight segments and further study five clear Lagrangian cases. They find indications of slow O_3 increases and CO decreases in the UT over the Atlantic.

[25] J. Al-Saadi et al. (unpublished manuscript, 2006) investigated source/receptor relationships to characterize the dominant contributions to O_3 distributions over the continental United States and Europe during the summer of 2004 campaign. For both United States and Europe they find that (1) approximately half the air in the lower troposphere (LT) experiences O_3 production within the domain upon exposure to local precursor emissions, (2) air influenced by the stratosphere and by strong mixing has origins primarily over the Pacific Ocean 10 days earlier, and (3) exposure to high levels of PAN in the midtroposphere characterizes 20–25% of all free tropospheric air. The largest differences between United States and Europe were associated with persistent deep convection over the Gulf of Mexico and southern United States. They find relatively little direct Asian influence on ozone over the United States during the summer of 2004 (2%) but a sizable U.S. influence on Europe (9%).

3.2. Composition and Chemistry in the North American Troposphere

[26] As can be seen from Figure 3, INTEX-A successfully characterized air masses of multiple origins over NA and the Atlantic at all different altitudes. Salient among these were pollution plumes from Alaskan fires and anthropogenic pollution, and stratospheric incursions in the UT. A number of papers in this special section analyze and interpret these observations.

3.2.1. Ozone

[27] Ozone was measured via in situ instruments and a UV lidar aboard the DC-8 as well as from coordinated ozonesonde launches from IONS (http://croc.gsfc.nasa.gov/intex/ions.html). The latter provided nearly 300 O_3 profiles from eleven North American sites and the R/V *Ronald H. Brown* in the Gulf of Maine [*Thompson et al.*, 2006a, 2006b]. Analysis of daily ozone soundings show that northeastern NA during INTEX-A was dominated by weak frontal systems that mixed aged pollution and stratospheric ozone with ozone from more recent pollution and lightning. These sources were quantified to give tropospheric ozone budgets for individual soundings. *Cooper et al.* [2006] utilize data from daily ozonesondes, commercial aircraft, and lidar at 14 sites during July-August 2004 and find that the UT above midlatitude eastern NA contained 15–16 ppb more tropospheric residual ozone than the UT at the westerly upwind sites, as well as the more polluted surface layers (0–2 km). Using observed data and simulations, they conclude that these O_3 enhancements can be generated from photochemical synthesis given significant amounts of lightning NO_x and only background mixing ratios of CO and VOCs.

3.2.2. Reactive Nitrogen

[28] INTEX-A provided the most detailed measurements of reactive nitrogen over the NA troposphere. *Singh et al.* [2006] analyze the distribution and partitioning of this group of chemicals. They find that the North American UT was greatly influenced by both lightning NO_x and surface pollution lofted via convection and contained elevated concentrations of PAN, ozone, hydrocarbons, and NO_x. Under polluted conditions PAN was a dominant carrier of reactive nitrogen in the UT, while HNO_3 dominated in the LT. Unknown alkyl nitrates appear to be present in the continental boundary layer in moderately large concentrations. L. W. Horowitz et al. (Observational constraints on the chemistry of isoprene nitrates over the eastern United States, submitted to *Journal of Geophysical Research*, 2006, hereinafter referred to as Horowitz et al., submitted manuscript, 2006) suggest that isoprene nitrate may be a major contributor. *Huey et al.* [2006] performed the first direct in situ measurements of HO_2NO_2 in the troposphere. The highest mean HO_2NO_2 mixing ratios (76 ppt) were observed at altitudes of 8–9 km, with lower levels above and below. CTMs capture the broad structure of HO_2NO_2 but uncertainties among models are quite large. Aerosol nitrate appeared to be mostly contained in large soil-based particles in the LT. Observational data suggested that lightning was a far greater contributor to NO_x in the UT than previously believed and a major source of uncertainty among models [*Singh et al.*, 2006; Hudman et al., submitted manuscript, 2006; Porter et al., unpublished manuscript, 2006]. J. E. Dibb et al. (unpublished manuscript, 2006) use Beryllium-7 and the HNO_3/O_3 ratio to identify similar distinct stratospheric and tropospheric populations in the UT. Estimates based on ^{7}Be suggest that the stratosphere was a major source of HNO_3 in the UT. Hudman et al. (submitted manuscript, 2006) and R. B. Pierce et al. (Chemical data assimilation based estimates of continental U.S. ozone and nitrogen budgets during INTEX-A, submitted to *Journal of Geophysical Research*, 2006, hereinafter referred to as Pierce et al., submitted manuscript, 2006) calculate a NO_y export efficiency of 16% and 24% respectively from eastern NA using two different models.

3.2.3. HO_x, Peroxides, and OVOC

[29] Measurements of OH and HO_2 in INTEX-A provided an excellent test of atmospheric oxidation chemistry in and out of pollution plumes throughout the troposphere. X. Ren et al. (unpublished manuscript, 2006) compared OH and HO_2 measurements to predictions using a photochemical box model constrained by coincident measurements of long-lived tracers and physical parameters. For most of the troposphere, observed OH and HO_2 were less than expected from model calculations (Figure 4). In the planetary boundary layer of forested regions, the observed-to-modeled OH ratio is a strong function of isoprene. The observed and modeled HO_2 greatly deviated in the UT ($\sim$2.5 at 11 km), implying, if the measurements are correct, a major flaw in current understanding of HO_x chemistry. These lower-than-expected OH measurements throughout much of the troposphere in northern midlatitudes have wide implications for ozone formation, global oxidation capacity, and reactive nitrogen distribution.

[30] Peroxides and formaldehyde were measured by two separate instruments [*Crounse et al.*, 2006; J. Snow et al., Hydrogen peroxide, methylhydroperoxide, and formaldehyde over North America and the North Atlantic, submitted to *Journal of Geophysical Research*, 2006, hereinafter referred to as Snow et al., submitted manuscript, 2006; A. Fried et al., unpublished manuscript, 2006]. Measurements of peroxides also revealed the presence of peroxyacetic acid (PAA), which was quantified for the first time in INTEX-A. On several flights, the concentration of PAA in the UT exceeded that of hydrogen peroxide. Simulations using a

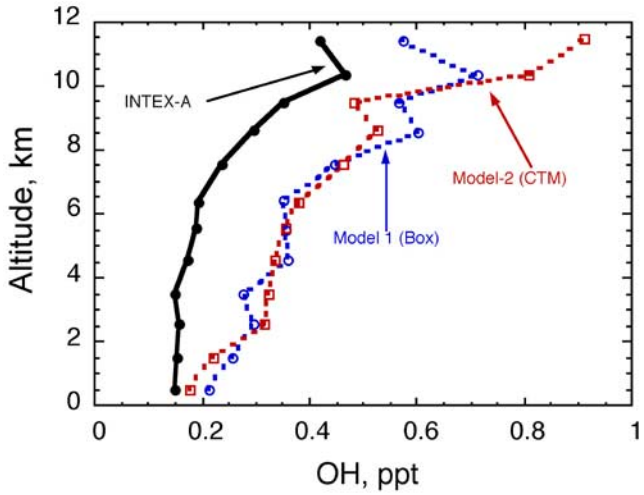

Figure 4. Observed and modeled OH mixing ratios in INTEX-A. Models 1 and 2 are the LaRC box model and the GEOS-Chem CTM, respectively. See Table 4 for more details. Data and model comparisons were performed over a single grid extending from 30–50°N and 260–320°W.

constrained box model greatly underestimated the observed concentrations of PAA. In the UT, PAA was often 10–100 times larger than expected (Crounse et al., submitted manuscript, 2006). Unusually high concentrations of formaldehyde in the UT support the role of rapid convection that lofted HCHO from the LT (A. Fried et al., unpublished manuscript, 2006). *Bertram et al.* [2006] find that convective outflow was strongest between 9 and 11 km and that more than 33% of the air in the UT had been placed there by convection within the last 2 days. Snow et al. (submitted manuscript, 2006) report considerable variability in mixing ratios of H_2O_2, CH_3OOH, and HCHO throughout the North American and North Atlantic troposphere. Convectively influenced air parcels were found to be enhanced in CH_3OOH, HCHO, CO, NO, and NO_2, while H_2O_2 and HNO_3 were depleted by wet removal. Biomass burning was also shown to increase UT H_2O_2, CH_3OOH, and HCHO mixing ratios even after 4–5 days of transit.

[31] Oxygenated volatile organic compounds (OVOC) comprise a large number of the species whose transport to the remote troposphere can impact radical budgets, sequester NO_x in the form of nitrates, and play a role in the formation of organic aerosols. *Kwan et al.* [2006] use measurements of atmospheric oxidants and aerosol size distributions performed on the DC-8 during INTEX-A to suggest that organic aerosol oxidation by OH can be a significant source of OVOC in the troposphere. They estimate that the potential magnitude of OVOC flux from organic aerosol to be as large as 70 ppt C/day in the free troposphere. The potential importance and highly uncertain nature of these estimates highlight the need for field and laboratory studies on organic aerosol composition and aging.

3.2.4. Aerosols and Radiation

[32] Clarke et al. (submitted manuscript, 2006) performed thermal analysis of aerosol size distributions and found that the "nonplume" regional haze was dominated by pollution characteristics near the surface and biomass burning aloft. Volatile OC included most water-soluble organic carbon. Refractory OC (stable at 400°C) dominated the enhanced shortwave absorption in plumes from Alaskan and Canadian forest fires. Biomass burning, pollution, and dust aerosol could be stratified by their combined spectral scattering and absorption properties. The measured response in light scattering to humidity revealed that ambient AOD typically included a 30–50% contribution from water due to its hygrosopicity.

[33] Dry aerosol mass measured on the lowest flight legs provided an estimate of PM2.5, such as would be measured at the surface. Y. Shinozuka et al. (Aircraft profiles of aerosol microphysics and optical properties over North America: Aerosol optical depth and its association with PM2.5 and water uptake, submitted to *Journal of Geophysical Research*, 2006) show that ambient column AOD is well correlated ($R^2 = 0.74$) to near surface PM2.5 for most cases. This indicates satellite measurements of AOD could be used as a surrogate for PM2.5 for regions over NA where such measurements are not currently available. A related study by S. Kondragunta et al. (unpublished manuscript, 2006) demonstrated that GOES AODs capture variability in atmospheric aerosol loading and can be used as a proxy to monitor pollution associated with urban/industrial sources and biomass burning events.

[34] Other INTEX-A measurements of aerosols and radiation from the J-31 have been reported by *Redemann et al.* [2006]. They found high variability in the derived aerosol forcing efficiencies for the visible wavelength range (350–700 nm). They also estimated aerosol absorption by matching calculations with the measured gradients of aerosol optical depth and radiant flux. In this way, they found larger aerosol absorption earlier in the 12 July to 8 August period, consistent with independent trajectory analyses and satellite imagery that showed the stronger influence of smoke aerosols from Alaska fires during the early period.

3.2.5. Carbon Cycle and CO_2

[35] North American terrestrial ecosystems are major sources and sinks of carbon. Quantifying their role in the continental carbon budget was a key objective in INTEX-A. Highly precise (±0.25 ppm), fast-response (1 s) measurements of CO_2 were obtained aboard the NASA DC-8 during INTEX-A. These measurements provided extensive regional-scale information on carbon sources and sinks over sparsely sampled areas of NA and adjacent ocean basins. Y. Choi et al. (unpublished manuscript, 2006) and K. Vadrevu et al. (unpublished manuscript, 2006) use airborne and satellite data along with models to investigate the ecosystem-atmospheric CO_2 exchange over NA and its relationship with the observed atmospheric variability of CO_2 resulting from biospheric uptake, industrial activity, and atmospheric dynamics. An example of the observed drawdown of CO_2 (approximately 3%) and short-term variability particularly in the free troposphere is shown in Figure 5a. Several products derived from the LANDSAT, NOAA AVHRR, and MODIS sensors were assimilated to specify spatiotemporal patterns of land use cover and vegetation characteristics to link the aircraft CO_2 data with terrestrial sources of carbon. They find that the lowest CO_2 mixing ratios were over agricultural fields in Illinois dominated by corn, a C_4 plant having a high photosynthetic rate.

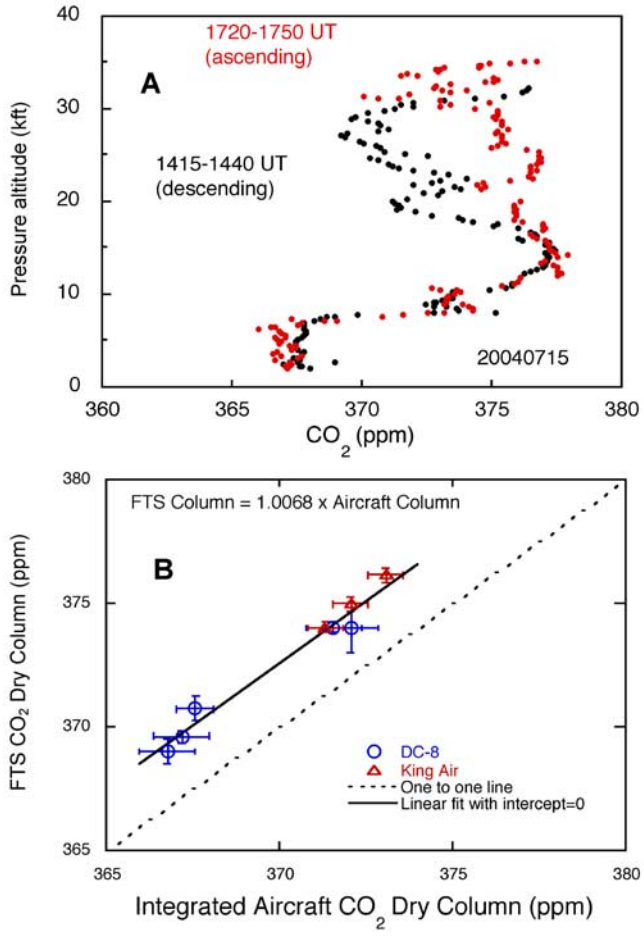

Figure 5. In situ and column CO_2 measurements during INTEX-A at the Wisconsin WLEF Tall Tower site (45.945°N, 90.273°W). (a) Vertical structure of CO_2 (15 July 2004) and short-term (3-hour) variability and (b) FTS column measurement comparison with in situ CO_2.

[36] To facilitate and test column measurements of CO_2 from ground-based and spaceborne instruments, the DC-8 and The University of Wyoming King Air aircraft (S. Wofsy, Harvard, concurrent COBRA campaign) recorded eight in situ CO_2 profiles over the Park Falls Wisconsin WLEF Tall Tower Site (45.945°N, 90.273°W) where an automated solar observatory for measuring atmospheric column abundances of CO_2 was colocated. Comparison of the integrated aircraft profiles and ground-based CO_2 column abundances (Figure 5b) showed excellent correlation but a small (0.7%) bias [*Washenfelder et al.*, 2006]. The comparison to aircraft integrated columns allowed the CO_2 retrievals to be corrected reducing the uncertainty in retrieved column average CO_2 mixing ratio to ~0.3% (±1.1 ppm).

3.3. Integrated Model Analysis of INTEX-A Observations

[37] INTEX-A provided a vast amount of observational data that was further analyzed with the help of a variety of models of chemistry and transport (Table 4). Figure 6 shows a comparison of the observed O_3 to NO_y ratio and its simulation by four state of the art models over a large grid over eastern NA (30–50°N; 260–320°W). This ratio is chosen to compare models as it requires simulations of both O_3 and its precursors (reactive nitrogen and hydrogen) and provides a qualitative measure of O_3 formation efficiency. It is evident that models disagree substantially with observations as well as with each other. Validation of existing models and their further improvement using INTEX-A data was a key focus in this campaign.

3.3.1. Synthesis of Results Using 3-D Models

[38] Pierce et al. (submitted manuscript, 2006) performed global ozone analyses, based on assimilation of stratospheric profile and ozone column measurements, and NO_y predictions from the RAQMS model to estimate the ozone and NO_y budget over the continental United States. Comparison with available observations show that RAQMS captured the main features of the global and continental U.S. distribution of tropospheric ozone, CO, and NO_y with reasonable fidelity. This study suggests that the majority of the continental U.S. export occurred in the UT/LS poleward of the tropopause break. Continental U.S. photochemically produced ozone was found to be a small component of the total ozone export, which was dominated by stratospheric ozone during INTEX-A. The NO_y export efficiency was estimated to be 24%, with NO_x and PAN together accounting for half of the total NO_y export.

[39] Hudman et al. (submitted manuscript, 2006) used the GEOS-Chem model to test current understanding of the regional budget of reactive nitrogen. They found that a 50% reduction in power plant and industry NO_x emissions over the eastern United States between 1999 and 2004 due to the NO_x abatement plans resulted in estimated ozone decreases of 1–6 ppb. Increasing the model lightning source to match the constraints of observed NO_x had a 5–10 ppb positive impact on free tropospheric O_3, but led to a significant overestimate of OH. A Lagrangian analysis of the fraction of North American emissions vented to the free troposphere using NO_y-CO correlations indicated an NO_y export fraction of 15% consistent with previous studies, but significantly lower than those estimated by Pierce et al. (submitted manuscript, 2006). They report that PAN was by far the

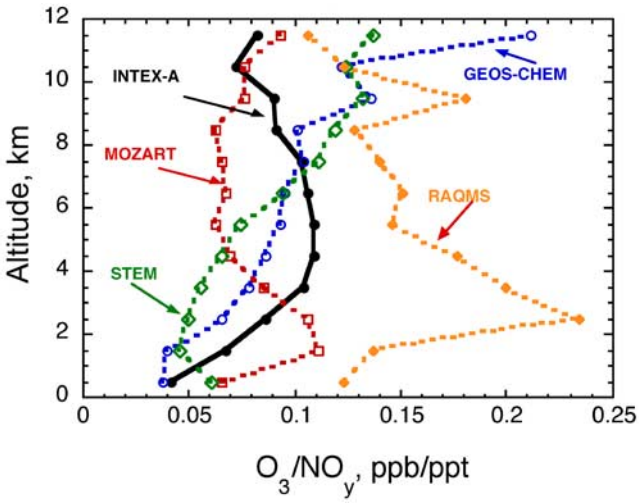

Figure 6. A comparison of observed and simulated O_3/NO_y ratios indicating uncertainties among four selected chemical transport models. Data and model domain were as in Figure 4.

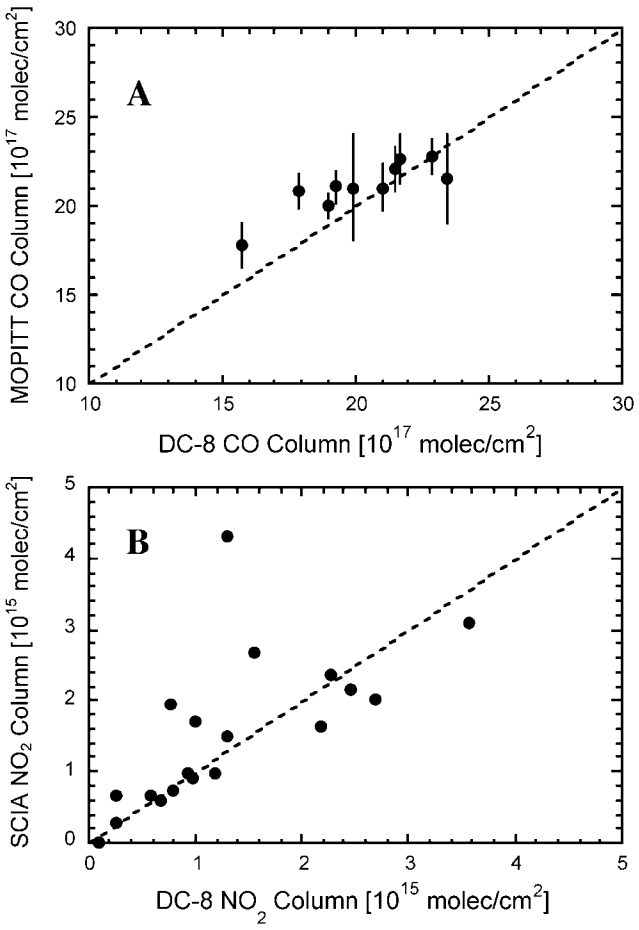

Figure 7. Comparison of (a) MOPITT CO and (b) SCIMACHY NO_2 tropospheric column retrievals with the INTEX-A DC-8 in situ profiles transformed by the corresponding averaging kernels.

dominant component of NO_y (>50%) in pollution plumes above 3.5 km.

[40] Horowitz et al. (submitted manuscript, 2006) used a CTM simulation (Table 4) in conjunction with INTEX-A total alkyl nitrate and isoprene observations over the eastern United States to constrain uncertainties in the chemistry of isoprene nitrates. The best agreement between simulated and observed boundary layer concentrations of organic nitrates was obtained with a 4% yield of isoprene nitrate production from the reaction of isoprene hydroperoxy radicals with NO, recycling of 40% NO_x when isoprene nitrates react with OH, and fast dry deposition of isoprene nitrates. Isoprene nitrates were shown to have a major impact on the NO_x budget in the continental boundary layer, consuming 17–21% of the emitted NO_x.

[41] *Pfister et al.* [2006] tested the MOZART-4 model with aircraft measurements and examined the ozone production from a case study of wildfires in Alaska and Canada. Modeled and observed enhancement ratios ($\Delta O_3/\Delta CO$) were about 0.25 ppb/ppb and resulted in a global net ozone production of 13 ± 2 Tg O_3 during summer 2004 in good agreement with the net ozone production calculated in the model for a region ranging from Alaska to the East Atlantic (9–11 Tg O_3). On average, the fires increased the ozone burden (surface–300 hPa) over Alaska and Canada during summer 2004 by about 7–9%, and over Europe by about 2–3%.

3.3.2. Model Evaluations

[42] S. Yu et al. (A comprehensive evaluation of the Eta-CMAQ forecast model performance for O_3, its related precursors, and meteorological parameters during the 2004 ICARTT study, submitted to *Journal of Geophysical Research*, 2006) tested the performance of Eta-CMAQ model forecasts with the surface observations available during this campaign. The model was able to capture the observed daily maximum 8-hour O_3 within a factor of 1.5 but underestimated CO by ~30% likely because of inadequate representation of the transport of pollution associated with Alaska forest fires. T. Chai et al. (Evaluating and improving regional emission estimates using the ICARTT observations, submitted to *Journal of Geophysical Research*, 2006) assimilated various O_3 measurements during INTEX-A/ICARTT into the STEM regional CTM and evaluated the effects of assimilating O_3 observations on model predictions. During the operational phase of the ICARTT field experiment in 2004, the regional air quality model STEM showed a strong positive surface bias, and a negative UT bias with respect to ozone (M. Mena-Carrasco et al., unpublished manuscript, 2006). After updating emissions from NEI 1999 to NEI 2001 (with a 2004 large point sources inventory update) and modifying boundary conditions, surface model bias was essentially eliminated. Observed and modeled ozone production efficiencies were in good agreement suggesting that the recurring ozone bias was due to overestimated NO_x emissions.

3.4. Satellite Validation During INTEX-A

[43] Figure 2 shows all the satellite spirals undertaken by the DC-8 during INTEX-A to validate principally AIRS (Aqua), MOPITT (Terra), and SCIAMACHY (Envisat) for CO, HCHO, NO_2, O_3 and H_2O. The three satellite sensors of primary attention for the J-31 aircraft were MISR on Terra, MODIS on Terra, and MODIS on Aqua and the focus was on validating satellite retrievals of AOD spectra and water vapor columns.

3.4.1. Chemistry-Based Validations

[44] W. W. McMillan et al. (unpublished manuscript, 2006) used DC-8 coincident CO data to provide crucial assessment of AIRS midtropospheric CO retrievals (400–500 hPa). They find that AIRS 400–500 hPa CO retrievals were biased high by approximately 8 (±5)%. *Emmons et al.* [2006] used INTEX-A and other available measurements of CO designed to be coincident with MOPITT overpasses for the continued validation of the CO retrievals from the MOPITT instrument onboard the Terra satellite. On average, MOPITT was 7–14% high at 700 hPa and 3% high at 350 hPa and generally consistent with the MOPITT design criteria of 10% accuracy. Figure 7 shows the agreement between MOPITT and DC-8 based CO columns in the troposphere. MOPITT is shown to be useful at describing CO during several meteorological scenarios involving Alaskan fires, urban plumes and a warm conveyor belt, in the middle to upper troposphere (C. M. Kiley et al., unpublished manuscript, 2006).

[45] A. Heckel et al. (unpublished manuscript, 2006) and *Martin et al.* [2006] compared coincident airborne in situ measurements of NO_2 from INTEX-A with those derived

from SCIAMACHY. A reasonable correlation was indicated although random errors of the order of 50% were possible (Figure 7). *Martin et al.* [2006] further analyzed SCIAMACHY and airborne NO_2 data to derive top-down emission estimates via inverse modeling using GEOS-Chem (Table 4). Their global emission inventory for land surface NO_x emissions (46 Tg N yr^{-1}) was 22% larger than the GEIA-based bottom-up inventory for 1998 but was shown to improve the GEOS-Chem simulation of NO_x, PAN, and HNO_3 over eastern NA. Although the Aura satellite was launched in July 2004 and not ready for validation during INTEX-A, Ozone-CO correlations observed in INTEX-A were compared to summer 2005 correlations observed by the Aura TES instrument in North American outflow as a test of the ability of TES to observe these constituents [*Zhang et al.*, 2006].

[46] *Millet et al.* [2006] performed a detailed error analysis to investigate if satellite retrieved HCHO columns from GOME (and OMI) could be used as a proxy for isoprene emissions over NA. They used aircraft data collected over NA and the Atlantic during INTEX-A and the GEOS-Chem model to draw conclusions about space-based mapping of VOC emissions. From observed HCHO and isoprene profiles they infer an HCHO molar yield from isoprene oxidation of 1.6 ± 0.5, consistent with current chemical mechanisms. Retrieval errors, combined with uncertainties in the HCHO yield from isoprene oxidation, resulted in an estimated 40% (1σ) error in inferring isoprene emissions from HCHO satellite measurements.

3.4.2. Optical Property–Based Validations

[47] *Russell et al.* [2006] report J-31 AOD measurements using AATS and compare them to retrievals by three satellite sensors: MISR on Terra and MODIS on both Terra and Aqua. Comparisons of MISR and AATS on days with strong AOD gradients over the Gulf of Maine showed that MISR (versions 15 and 16) captured the AATS-measured AOD gradient ($R^2 = 0.9$) for all 4 MISR wavelengths (446 to 866 nm). Comparisons of MODIS and AATS AOD values on 8 overpasses using 61 grid cells yielded $R^2 = 0.97$ and RMS difference = 0.03, with about 87% of the MODIS AOD retrievals agreeing with AATS values within the MODIS over-ocean uncertainty. In contrast the MODIS-AATS differences in Ångstrom exponent (−dlnAOD/dlnl) were rather large but improved substantially when cases with small AOD (<0.1 at 855 nm) were excluded. Water vapor measurements from AATS were in good agreement with those of the in situ Vaisala HMP243 sensor and sondes (J. Livingston et al., Comparison of water vapor measurements by airborne sunphotometer and near-coincident in situ and satellite sensors during INTEX-A 2004, submitted to *Journal of Geophysical Research*, 2006). However, MODIS infrared retrievals of column water vapor were poorly correlated with ($R^2 = 0.20$) and significantly exceeded those of AATS. In comparison, AIRS layer water vapor agreed with AATS and Vaisala to within 10%.

[48] S. Kondragunta et al. (unpublished manuscript, 2006) determined that operational GOES AOD imagery provided accurate spatial extent of pollution plumes despite residual cloud contamination in certain pixels. Although the GOES-suborbital AOD differences were notably larger than MODIS-suborbital differences reported by *Russell et al.* [2006] and others, S. Kondragunta et al. (unpublished manuscript, 2006) argue that that GOES AODs are a good proxy to monitor pollution associated with urban/industrial sources and biomass burning events. Results from these INTEX-A validation studies are helping to quantify the tradeoffs between the greater frequency of GOES retrievals from a geostationary operational satellite and the greater accuracy of more modern sensors on polar orbiting satellites such as MODIS and MISR.

4. Conclusion

[49] These INTEX-A/ICARTT measurements provide a rich data set for describing the composition and chemistry of the North American troposphere, for investigating the transformation of gases and aerosols during long-range transport, for the radiation balance of the troposphere, and for validating a variety of satellite observations as well as models of chemistry and transport. Some of the highlights of this study include the first airborne measurements of HO_2NO_2 and peroxyacetic acid, successful conduct of quasi-Lagrangian studies to investigate processes of chemical aging during transatlantic transport, characterization of Asian pollution over NA in the summer, and the finding of an unexpectedly large source of lightning NO_x in the troposphere. The oxidation capacity of atmosphere, determined by the observed HO_x concentrations, was found to be nearly a factor of two lower than predicted by models. The results presented in this special section of JGR represent only the initial analysis, and much more integrated analysis is expected in the near future. The data are available to all interested parties for further analysis.

Notation

AATS	Ames Airborne Tracking Sunphotometer.
AERONET	Aerosol Robotic Network.
AIRS	Atmospheric Infrared Sounder.
AOD	Aerosol optical depth.
AVHRR	Advanced very high resolution radiometer.
CIMS	Chemical ionization mass spectrometry.
CMAQ	Community multiscale air quality.
CTM	Chemical transport model.
DLR	Deutschen Zentrum für Luft- und Raumfahrt.
FTS	Fourier Transform Spectrometer.
GOES	Geostationary Operational Environmental Satellite.
ICARTT	International Consortium for Atmospheric Research on Transport and Transformation.
INTEX-A	Phase 1 of INTEX-NA.
INTEX-B	Phase 2 of INTEX-NA.
INTEX-NA	Intercontinental Chemical Transport Experiment–North America.
IONS	INTEX Ozonesonde Network Study.
LIF	Laser induced fluorescence.
LIS	Lightning imaging sensor.
LRLN	Long-Range Lightning Network.
LS	Lower stratosphere.
LT	Lower troposphere.
MISR	Multiangle Imaging SpectroRadiometer.
MODIS	Moderate Resolution Imaging Spectroradiometer.

MOPITT	Measurement of Pollution in the Troposphere.
MOZAIC	Measurement of Ozone on Airbus In-service Aircraft.
MOZART	Model of Ozone and Related Tracers.
NA	North America.
NASA	National Aeronautics and Space Administration
NCEP	National Centers for Environmental Prediction.
NOAA	National Oceanic and Atmospheric Administration.
NLDN	National Lightning Detection Network.
OC	Organic carbon.
OMI	Ozone monitoring instrument.
OVOC	Oxygenated volatile organic chemicals.
PANs	Peroxy acetyl nitrates.
RAQMS	Real-Time Air Quality Modeling System.
SCIAMACHY	Scanning Imaging Absorption Spectrometer For Atmospheric Chartography.
SSFR	Solar Spectral Flux Radiometer.
STEM	Sulfur Transport and Deposition Model.
TDL	Tunable Diode Laser.
TES	Tropospheric Emission Spectrometer.
TOMCAT	Toulouse Offline Model of Chemistry and Transport.
TOMS	Total Ozone Measuring Spectrometer.

[50] **Acknowledgments.** We thank all ICARTT participants and sponsoring agencies for making this project possible. DC-8 activities were supported by the NASA Tropospheric Chemistry Program. J-31 activities received partial support from NASA's Radiation Science and NOAA's Atmospheric Composition and Climate Programs. We very much appreciate the dedicated efforts of all personnel associated with DC-8 activities from NASA Dryden, NASA Wallops, University of North Dakota, and J-31 personnel from Sky Research in making this campaign a success.

References

Bertram, T. H., et al. (2006), Direct measurements of the convective recycling of the upper troposphere, *Science*, in press.

Borrell, P., P. M. Borrell, J. P. Burrows, and U. Platt (Eds.) (2004), *Sounding the Troposphere From Space: A New Era for Atmospheric Chemistry*, pp. 1–446, Springer, New York.

Cook, P., et al. (2006), Forest fire plumes over the North Atlantic: p-TOMCAT model simulations with aircraft and satellite measurements from the ITOP/ICARTT campaign, *J. Geophys. Res.*, doi:10.1029/2006JD007563, in press.

Cooper, O. R., et al. (2006), Large upper tropospheric ozone enhancements above mid-latitude North America during summer: In situ evidence from the IONS and MOZAIC ozone monitoring network, *J. Geophys. Res.*, *111*, D24S05, doi:10.1029/2006JD007306.

Crawford, J. H., et al. (1999), Assessment of upper tropospheric HOx sources over the tropical Pacific based on NASA GTE/PEM data: Net effect on HO_x and other photochemical parameters, *J. Geophys. Res.*, *104*, 16,255–16,273.

Crounse, J. D., K. A. McKinney, A. J. Kwan, and P. O. Wennberg (2006), Measurement of gas-phase hydroperoxides by chemical ionization mass spectrometry (CIMS), *Anal. Chem.*, in press.

Day, D. A., P. J. Wooldridge, M. B. Dillon, J. A. Thornton, and R. C. Cohen (2002), A thermal dissociation laser-induced fluorescence instrument for in situ detection of NO_2, peroxy nitrates, alkyl nitrates, and HNO_3, *J. Geophys. Res.*, *107*(D6), 4046, doi:10.1029/2001JD000779.

Derwent, R. G., et al. (2006), External influences on Europe's air quality: Baseline methane, carbon monoxide and ozone from 1990 to 2030 at Mace Head, Ireland, *Atmos. Environ.*, *40*(5), 844–855.

Emmons, L. K., et al. (2006), MOPITT validation exercises during summer 2004 field campaigns over North America, *J. Geophys. Res.*, doi:10.1029/2006JD007833, in press.

Fehsenfeld, F. C., M. Trainer, D. D. Parrish, A. Volz-Thomas, and S. Penkett (1996), North Atlantic Regional Experiment 1993 summer intensive: Foreword, *J. Geophys. Res.*, *101*(D22), 28,869–28,875.

Fehsenfeld, F. C., et al. (2006), International Consortium for Atmospheric Research on Transport and Transformation (ICARTT): North America to Europe—Overview of the 2004 summer study, *J. Geophys. Res.*, doi:10.1029/2006JD007829, in press.

Grousset, F. E., P. Ginoux, A. Bory, and P. E. Biscaye (2003), Case study of a Chinese dust plume reaching the French Alps, *Geophys. Res. Lett.*, *30*(6), 1277, doi:10.1029/2002GL016833.

Guerova, G., I. Bey, J.-L. Attie, R. V. Martin, J. Cui, and M. Sprenger (2006), Impact of transatlantic transport episodes on summertime ozone in Europe, *Atmos. Chem. Phys.*, *6*, 2057–2072.

Hoell, J. M., D. D. Davis, S. C. Liu, R. Newell, M. Shipham, H. Akimoto, R. J. McNeal, R. J. Bendura, and J. W. Drewry (1996), Pacific Exploratory Mission–West A (PEM-West A): September–October 1991, *J. Geophys. Res.*, *101*, 1641–1653.

Hoell, J. M., D. D. Davis, S. C. Liu, R. E. Newell, H. Akimoto, R. J. McNeal, and R. J. Bendura (1997), The Pacific Exploratory Mission–West Phase B: February–March 1994, *J. Geophys. Res.*, *102*, 28,223–28,239.

Holloway, T., A. M. Fiore, and M. G. Hastings (2003), Intercontinental transport of air pollution: Will emerging science lead to a new hemispheric treaty?, *Environ. Sci. Technol*, *37*, 4535–4542.

Horowitz, L. W., et al. (2003), A global simulation of tropospheric ozone and related tracers: Description and evaluation of MOZART, version 2, *J. Geophys. Res.*, *108*(D24), 4784, doi:10.1029/2002JD002853.

Houghton, J. T., et al. (2001), *Climate Change 2001: The Scientific Basis*, Cambridge Univ. Press, New York.

Huey, L. G., et al. (2006), Measurement of HO_2NO_2 in the upper troposphere during INTEX-NA 2004, *J. Geophys. Res.*, doi:10.1029/2006JD007676, in press.

Huntrieser, J., et al. (2006), Intercontinental air pollution transport from North America to Europe: Experimental evidence from airborne measurements and surface observations, *J. Geophys. Res.*, *110*, D01305, doi:10.1029/2004JD005045.

Jacob, D. J., J. Logan, and P. Murti (1999), Effect of rising Asian emissions on surface ozone in the United States, *Geophys. Res. Lett.*, *26*, 2175–2178.

Jacob, D. J., J. H. Crawford, M. M. Kleb, V. S. Connors, R. J. Bendura, J. L. Raper, G. W. Sachse, J. C. Gille, L. Emmons, and C. L. Heald (2003), Transport and Chemical Evolution over the Pacific (TRACE-P) aircraft mission: Design, execution, and first results, *J. Geophys. Res.*, *108*(D20), 9000, doi:10.1029/2002JD003276.

Jaffe, D., et al. (1999), Transport of Asian air pollution to North America, *Geophys. Res. Lett.*, *26*(6), 711–714.

Jaffe, D., H. Price, D. Parrish, A. Goldstein, and J. Harris (2003), Increasing background ozone during spring on the west coast of North America, *Geophys. Res. Lett.*, *30*(12), 1613, doi:10.1029/2003GL017024.

Kiley, C. M., and H. E. Fuelberg (2006), An examination of summertime cyclone transport processes during INTEX-A, *J. Geophys. Res.*, *111*, D24S06, doi:10.1029/2006JD007115.

Kwan, A. J., et al. (2006), On the flux of oxygenated volatile organic compounds from organic 3 aerosol oxidation, *Geophys. Res. Lett.*, *33*, L15815, doi:10.1029/2006GL026144.

Law, K., et al. (2005), Evidence for long-range transport of North American anthropogenic and wildfire emissions to Europe from airborne and ground based lidar measurements during European ITOP (IGAC Lagrangian 2K4, ICARTT), *Eos Trans. AGU*, *86*(52), Fall Meet. Suppl., Abstract A41D-01.

Lelieveld, J., et al. (2002), Global air pollution crossroads over the Mediterranean, *Science*, *298*, 794–799.

Lin, C.-Y. C., D. J. Jacob, J. W. Munger, and A. M. Fiore (2000), Increasing background ozone in surface air over the United States, *Geophys. Res. Lett.*, *27*, 3465–3468.

Liu, H., D. J. Jacob, L. Y. Chan, S. J. Oltmans, I. Bey, R. M. Yantosca, J. M. Harris, B. N. Duncan, and R. V. Martin (2002), Sources of tropospheric ozone along the Asian Pacific Rim: An analysis of ozonesonde observations, *J. Geophys. Res.*, *107*(D21), 4573, doi:10.1029/2001JD002005.

Martin, R. V., C. E. Sioris, K. Chance, T. B. Ryerson, T. H. Bertram, P. J. Wooldridge, R. C. Cohen, J. A. Neuman, A. Swanson, and F. M. Flocke (2006), Evaluation of space-based constraints on global nitrogen oxide emissions with regional aircraft measurements over and downwind of eastern North America, *J. Geophys. Res.*, *111*, D15308, doi:10.1029/2005JD006680.

Methven, J., et al. (2006), Establishing Lagrangian connections between observations within air masses crossing the Atlantic during the International Consertium for Atmospheric Research on Transport and Transformation experiment, *J. Geophys. Res.*, *111*, D23S62, doi:10.1029/2006JD007540.

Millet, D. B., et al. (2006), Formaldehyde distribution over North America: Implications for satellite retrievals of formaldehyde columns and isoprene emission, *J. Geophys. Res.*, *111*, D24S02, doi:10.1029/2005JD006853.

Oltmans, S. J., et al. (2006), Long-term changes in tropospheric ozone, *Atmos. Environ.*, *40*(17), 3156–3173.

Parrish, D. D., et al. (2004), Changes in the photochemical environment of the temperate North Pacific troposphere in response to increased Asian emissions, *J. Geophys. Res.*, *109*, D23S18, doi:10.1029/2004JD004978.

Pfister, G., P. G. Hess, L. K. Emmons, J.-F. Lamarque, C. Wiedinmyer, D. P. Edwards, G. Pétron, J. C. Gille, and G. W. Sachse (2005), Quantifying CO emissions from the 2004 Alaskan wildfires using MOPITT CO data, *Geophys. Res. Lett.*, *32*, L11809, doi:10.1029/2005GL022995.

Pfister, G., et al. (2006), Ozone production from boreal forest fire emissions, *J. Geophys. Res.*, doi:10.1029/2006JD007695, in press.

Pierce, R. B., et al. (2003), Regional Air Quality Modeling System (RAQMS) predictions of the tropospheric ozone budget over east Asia, *J. Geophys. Res.*, *108*(D21), 8825, doi:10.1029/2002JD003176.

Raper, J. L., M. M. Kleb, D. J. Jacob, D. D. Davis, R. E. Newell, H. E. Fuelberg, R. J. Bendura, J. M. Hoell, and R. J. McNeal (2001), Pacific Exploratory Mission in the tropical Pacific: PEM-Tropics B, March–April 1999, *J. Geophys. Res.*, *106*, 32,401–32,425.

Redemann, J., et al. (2006), Airborne measurements of spectral direct aerosol radiative forcing in the Intercontinental chemical Transport Experiment/Intercontinental Transport and Chemical Transformation of anthropogenic pollution, 2004, *J. Geophys. Res.*, *111*, D14210, doi:10.1029/2005JD006812.

Richter, A., J. P. Burrows, H. Nü, C. Granier, and U. Niemeier (2005), Increase in tropospheric nitrogen dioxide over China observed from space, *Nature*, *437*, 129–132.

Russell, P. B., P. V. Hobbs, and L. L. Stowe (1999), Aerosol properties and radiative effects in the United States east coast haze plume: An overview of the Tropospheric Aerosol Radiative Forcing Observational Experiment (TARFOX), *J. Geophys. Res.*, *104*(D2), 2213–2222.

Russell, P. B., et al. (2006), Multi-grid-cell validation of satellite aerosol property retrievals in INTEX/ITCT/ICARTT 2004, *J. Geophys. Res.*, doi:10.1029/2006JD007606, in press.

Schere, K. L., G. M. Hidy, and H. B. Singh (Eds.) (2000), *The NARSTO Ozone Assessment—Critical Reviews*, *Atmos. Environ.*, *34* (12–14).

Schoeberl, M. R., et al. (2004), Earth observing system missions benefit atmospheric research, *Eos Trans. AGU*, *85*(18), 177.

Simmonds, P. G., R. G. Derwent, A. L. Manning, and G. Spain (2004), Significant growth in surface ozone at Mace Head, Ireland, 1987–2003, *Atmos. Environ.*, *38*(28), 4769–4778.

Singh, H. B., A. Thompson, and H. Schlager (1999), SONEX airborne mission and coordinated POLINAT-2 activity: Overview and accomplishments, *Geophys. Res. Lett.*, *26*, 3053–3056.

Singh, H. B., D. J. Jacob, L. Pfister, and J. H. Crawford (2002), INTEX-NA: Intercontinental Chemical Transport Experiment-North America, December 2002, NASA Ames Res. Cent., Moffett Field, Calif. (Available at http://cloud1.arc.nasa.gov)

Singh, H. B., et al. (2006), Reactive nitrogen distribution and partitioning in the North American troposphere and lowermost stratosphere, *J. Geophys. Res.*, doi:10.1029/2006JD007664, in press.

Stohl, A., (Ed.) (2004), *Intercontinental Transport of Air Pollution, The Handbook of Environmental Chemistry*, 320 pp., Springer, New York.

Stohl, A., and T. Trickl (1999), A textbook example of long-range transport: Simultaneous observation of ozone maxima of stratospheric and North American origin in the free troposphere over Europe, *J. Geophys. Res.*, *104*, 30,445–30,462.

Tang, Y., et al. (2004), Three-dimensional simulations of inorganic aerosol distributions in east Asia during spring 2001, *J. Geophys. Res.*, *109*, D19S23, doi:10.1029/2003JD004201.

Thompson, A. M., et al. (2006a), IONS (INTEX Ozonesonde Network Study, 2004): 1. Perspective on summertime UT/LS (upper troposphere/lower stratosphere) ozone over northeastern North America, *J. Geophys. Res.*, doi:10.1029/2006JD007441, in press.

Thompson, A. M., et al. (2006b), IONS (INTEX Ozonesonde Network Study, 2004): 2. Tropospheric ozone budgets and variability over northeastern North America, *J. Geophys. Res.*, doi:10.1029/2006JD007670, in press.

VanCuren, R. A. (2003), Asian aerosols in North America: Extracting the chemical composition and mass concentration of the Asian continental aerosol plume from long term aerosol records in the western United States, *J. Geophys. Res.*, *108*(D20), 4623, doi:10.1029/2003JD003459.

Vingarzan, R. (2004), A review of surface ozone background levels and trends, *Atmos. Environ.*, *38*(21), 3431–3442.

Washenfelder, R. A., G. C. Toon, J.-F. Blavier, Z. Yang, N. T. Allen, P. O. Wennberg, S. A. Vay, D. M. Matross, and B. C. Daube (2006), Carbon dioxide column abundances at the Wisconsin Tall Tower site, *J. Geophys. Res.*, *111*, D22305, doi:10.1029/2006JD007154.

Wild, O., P. Pochanart, and H. Akimoto (2004), Trans-Eurasian transport of ozone and its precursors, *J. Geophys. Res.*, *109*, D11302, doi:10.1029/2003JD004501.

Zhang, L., et al. (2006), Continental outflow of ozone pollution as determined by O_3-CO correlations from the TES satellite instrument, *Geophys. Res. Lett.*, *33*, L18804, doi:10.1029/2006GL026399.

W. H. Brune, Department of Meteorology, Pennsylvania State University, University Park, PA 16902, USA.

J. H. Crawford, NASA Langley Research Center, Hampton, VA 23665, USA.

D. J. Jacob, Division of Applied Sciences, Harvard University, Cambridge, MA 02138, USA.

P. B. Russell and H. B. Singh, NASA Ames Research Center, Moffett Field, CA 94035, USA. (hanwant.b.singh@nasa.gov)